

A. R. Kerr
NASA Goddard Institute for Space Studies, New York, N. Y. 10025

Abstract

The theory of noise and frequency conversion in two-diode mixers is presented. The diodes are assumed to have non-linear conductance and capacitance, series resistance, and shot and thermal noise. The series resistance can include a frequency dependent skin-effect component. Any linear embedding network is allowed. Computed examples are given showing the effect of the loop inductance in subharmonically pumped mixers.

Introduction

Recent results^{1, 2} have demonstrated that subharmonically pumped mixers using an anti-parallel diode pair are comparable in performance with single-diode fundamental mixers, at least up to 100 GHz. The development of two-diode mixers has mainly been empirical, largely because, hitherto, no accurate theory of noise and frequency conversion has been available.

Two circuit parameters in the subharmonically pumped mixer are relatively easily controlled, namely: (i) the inductance in series with each diode, which strongly affects the loop currents, both small-signal and large-signal, circulating through the anti-parallel diodes; and (ii) the diode capacitance. It was the need to understand the effects of these parameters, and also the noise properties of two-diode mixers that stimulated the work reported here.

The method of analysis of the two-diode mixer uses a generalization of a recently published theory of single-diode mixers³ and is based on the fundamental small-signal conversion theory of Torrey and Whitmer⁴ and the noise theories of Dragone⁵ and Twiss⁶.

Small-Signal Analysis

Consider the two-diode mixer shown in Fig. 1. Each pumped diode can be represented as a multi-frequency multiport network, connected to an embedding network which is also a multi-frequency multi-port, as shown in Fig. 2. Representing the pumped diodes by their conversion admittance matrices \underline{Y}^A and \underline{Y}^B of size $(N \times N)$ and the embedding network by its admittance matrix \underline{Y}^E of size $(3N \times 3N)$, the complete mixer admittance \underline{Y}^M can be obtained by addition of the separate admittance matrices, corresponding to parallel connection of the networks. Thus, partitioning \underline{Y}^E into nine $(N \times N)$ submatrices, and adding the diode conversion admittance matrices

$$\underline{Y}^E = \begin{bmatrix} \underline{Y}_{AA}^E & \underline{Y}_{AB}^E & \underline{Y}_{AC}^E \\ \underline{Y}_{BA}^E & \underline{Y}_{BB}^E & \underline{Y}_{BC}^E \\ \underline{Y}_{CA}^E & \underline{Y}_{CB}^E & \underline{Y}_{CC}^E \end{bmatrix} \quad (1)$$

$$\text{and } \underline{Y}^M = \begin{bmatrix} \underline{Y}_{AA}^A + \underline{Y}_{AA}^E & \underline{Y}_{AB}^E & \underline{Y}_{AC}^E \\ \underline{Y}_{BA}^E & \underline{Y}_{BB}^B + \underline{Y}_{BB}^E & \underline{Y}_{BC}^E \\ \underline{Y}_{CA}^E & \underline{Y}_{CB}^E & \underline{Y}_{CC}^E \end{bmatrix}. \quad (2)$$

All the small signal properties of the mixer can be deduced from the mixer impedance matrix

$$\underline{Z}^M \triangleq (\underline{Y}^M)^{-1}. \quad (3)$$

The conversion loss from frequency $\omega_k = \omega_0 + k\omega_p$ to the IF ω_0 is given by

$$L_{0,k} = \frac{1}{4 |Z_{(C,0)(C,k)}^M|^2 \operatorname{Re}[Y_k] \operatorname{Re}[Y_0]} \quad (4)$$

where $Z_{(C,0)(C,k)}^M$ is the element of \underline{Z}^M in the row corresponding to the IF output port $(C,0)$ in Fig. 2, and the column corresponding to the signal input port (C,k) . Y_k and Y_0 are the signal source and IF load admittances, as shown in Fig. 2.

The input impedance Z_{in_k} seen by the source (or load) admittance Y_k is

$$Z_{in_k} = \left[\frac{1}{Z_{(C,k)(C,k)}^M} - Y_k \right]^{-1} \quad (5)$$

Noise Analysis

The shot noise in a periodically pumped diode exhibits partial correlation between all frequency components separated by a multiple of the pump frequency ω_p . Dragone⁵ has shown that the properties of this noise are concisely described by a noise-current correlation matrix having elements corresponding to every pair of sideband frequencies. For a two-diode mixer it can be shown that, although this partial correlation is present in the shot noise of each diode, there is no correlation between the shot noise of the two diodes*. However, the noise in diode A is coupled via the embedding network to diode B and vice-versa.

Thermal noise generated in the series resistances of the diodes and in loss in the mixer mount can be represented by equivalent noise current sources at each port of the 3N-port embedding network. These noise current sources are partially correlated. Twiss⁶ has shown that for a lossy reciprocal network whose admittance matrix is \underline{Y} , the elements of the noise current correlation matrix are

$$N_{mn} = 4kT \operatorname{Re}[Y_{mn}] \Delta f. \quad (6)$$

In characterizing our mixer, noise from the external signal, image, and IF terminations should be excluded. It is therefore convenient to define \underline{Y}^E (unterm.) as the admittance matrix of the embedding network with the appropriate source and load conductances $\operatorname{Re}[Y_k] = 0$.

Consider now the following noise current sources connected to the 3N ports of the whole mixer (Fig. 2): at ports (A,k) shot noise from diode A and thermal noise from the embedding network, at ports (B,k) shot noise from diode B

* This will be shown in a paper to be published shortly.

and thermal noise from the embedding network, and at ports (C, k) thermal noise from the embedding network only. The noise current correlation matrix \underline{N} (including both shot and thermal noise) has the general element $N_{(X,m)(Y,n)} \triangleq \langle \delta I_{N(X,m)} \delta I_{N(Y,n)}^* \rangle$ where $\delta I_{N(X,m)}$ and $\delta I_{N(Y,n)}$ are the total (shot and thermal) pseudosinusoidal noise current sources connected at ports (X, m) and (Y, n) in Fig. 2. From the work of Dragone and Twiss it follows that

$$N_{(A,m)(A,n)} = 2q I_{m-n}^A \Delta f + 4kT \operatorname{Re} \left[Y_{(A,m)(A,n)}^E \right] \Delta f \quad (7a)$$

$$N_{(B,m)(B,n)} = 2q I_{m-n}^B \Delta f + 4kT \operatorname{Re} \left[Y_{(B,m)(B,n)}^E \right] \Delta f \quad (7b)$$

where I_{m-n}^A and I_{m-n}^B are the (m-n)-th Fourier coefficients of the large-signal currents in the diode conductances. For all other combinations of values (A, B, or C) of X and Y

$$N_{(X,m)(Y,n)} = 4kT \operatorname{Re} \left[Y_{(X,m)(Y,n)}^E \right] \Delta f \quad (7c)$$

Let $\underline{Z}_{(C,0)}^M$ denote the output row (C, 0) of matrix \underline{Z}^M . The equivalent (single-sideband) input noise temperature of the mixer is then

$$T_M = \frac{\underline{Z}_{(C,0)}^M \underline{N} \underline{Z}_{(C,0)}^{M\dagger}}{4k \operatorname{Re} [Y_n] \cdot |Z_{(C,0)(C,n)}^M|^2 \Delta f} \quad (8)$$

Results

The above theory has been used to compute the performance of a number of subharmonically pumped and balanced mixers. For want of space only two examples will be given here, both subharmonically pumped mixers with the simple lumped element circuit of Fig. 3. In example 1 the impedance Z_L is zero at all frequencies above the signal and image, while in example 2 Z_L is a high impedance for these frequencies. The performance is shown in Figs. 4 and 5 as a function of the loop inductance L_S . The signal, pump, and IF are at 103, 50, and 3 GHz. Up to the signal frequency Z_L is 50Ω , except at the IF where it matches the output impedance of the mixer. The diode parameters are: $R_S = 10\Omega$, $C_0 = 7fF$, $\eta = 1.12$, $\phi = 0.95V$, $\gamma = 0.5$, $i_0 = 8 \times 10^{-17} A$. In all cases the LO power was adjusted to give a rectified current of 2 mA in each diode.

For each value of L_S , the conductance and capacitance waveforms were determined using a modification of the method described in ref. 7. The mixer performance was then calculated using (4), (5), and (8). Terms up to the eighth pump harmonic were included in \underline{Y}^A and \underline{Y}^B , resulting in size 27×27 matrices \underline{Y}^M and \underline{Z}^M .

The most interesting features of the results in Figs. 4 and 5 are the strong peaks in the conversion loss and noise. These appear largely to be governed by the ringing of the circuit while the diodes are not conducting. The largest peaks correspond to a second period of conduction because of a resonance between the diode capacitance and loop inductance near $2\omega_p$, and the smaller peaks correspond to circuit resonances near higher pump harmonics; for the latter there is usually no additional conduction period.

Acknowledgements

The author thanks P. H. Siegel for his help in developing a reliable method for computing the diode waveforms, and Alison V. Smith for her assistance with the computer programming.

References

1. E. R. Carlson, M. V. Schneider, and T. F. McMaster, "Subharmonically Pumped Millimeter-Wave Mixers", Trans. Microwave Theory Tech., Vol. MTT-26, No. 10, pp. 706-715, Oct. 1978.
2. T. F. McMaster, M. V. Schneider, and W. W. Snell, "Millimeter-Wave Receivers with Subharmonic Pump", IEEE Trans. Microwave Theory Tech., Vol. MTT-24, No. 12, pp. 948-952, Dec. 1978.
3. D. N. Held and A. R. Kerr, "Conversion Loss and Noise of Microwave and Millimeter-Wave Mixers: Part 1 - Theory and ... Part 2 - Experiment", IEEE Trans. Microwave Theory Tech., Vol. MTT-26, No. 2, pp. 49-61, Feb. 1978.
4. H. C. Torrey and C. A. Whitner, "Crystal Rectifiers", (MIT Radiation Lab. Series, Vol. 15), New York: McGraw-Hill, 1948.
5. C. Dragone, "Analysis of Thermal and Shot Noise in Pumped Resistive Diodes", Bell Syst. Tech. J., Vol. 47, pp. 1883-1902, Nov. 1968.
6. R. Q. Twiss, "Nyquist's and Thévenin's Theorems Generalized for Nonreciprocal Linear Networks", J. Appl. Phys., Vol. 26, No. 5, pp. 599-602, May 1955. See also E. J. Schremp in Ch. 12 of "Vacuum Tube Amplifiers", G. E. Valley and H. Wallman, Editors, (Vol. 18 of MIT Radiation Lab. Series), New York: McGraw-Hill 1948.
7. A. R. Kerr, "A Technique for Determining the Local Oscillator Waveforms in a Microwave Mixer", IEEE Trans. Microwave Theory Tech., Vol. MTT-23, No. 10, pp. 828-831, Oct. 1975.
8. P. H. Siegel and A. R. Kerr, to be published.

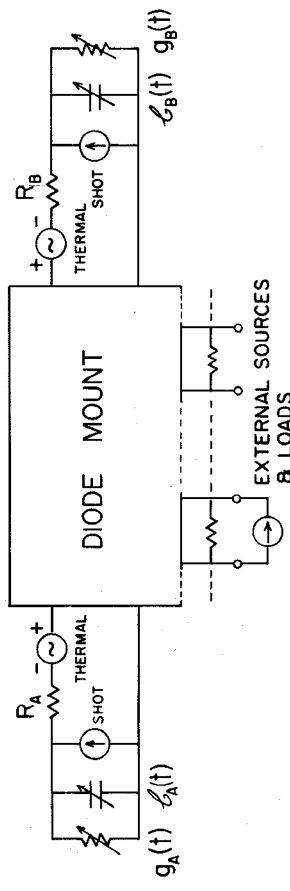


Fig. 1. Circuit of the two-diode mixer.

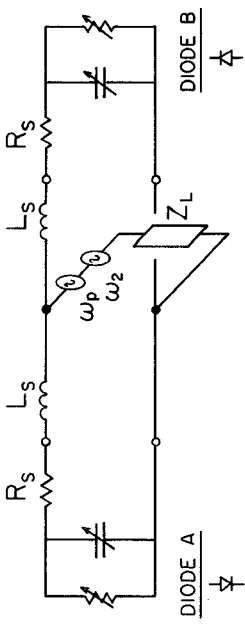


Fig. 3. Subharmonically pumped mixer used in examples 1 and 2.

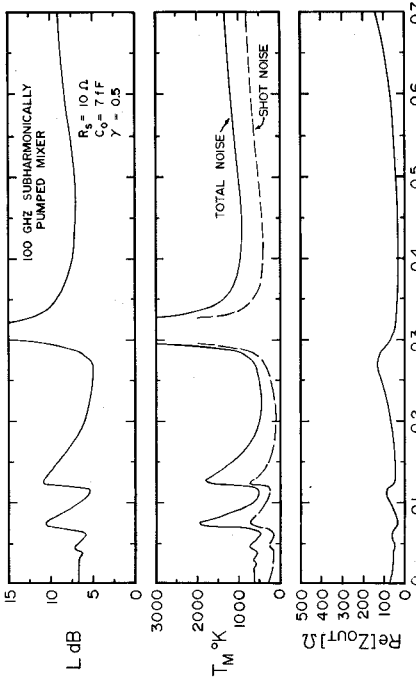


Fig. 4. Ex. 1. Z_L zero above signal frequency.

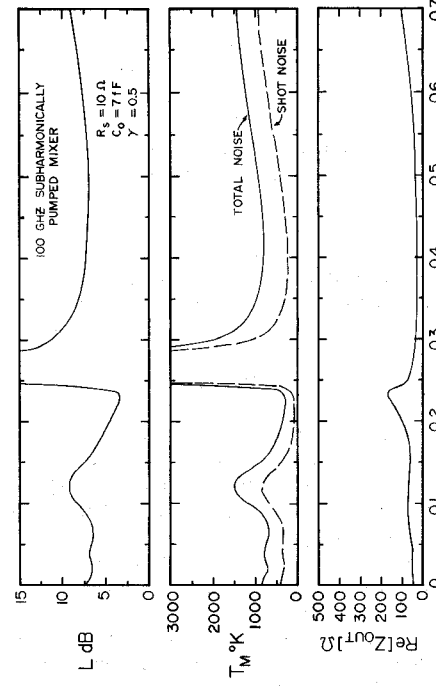


Fig. 5. Ex. 2. Z_L large above signal frequency.

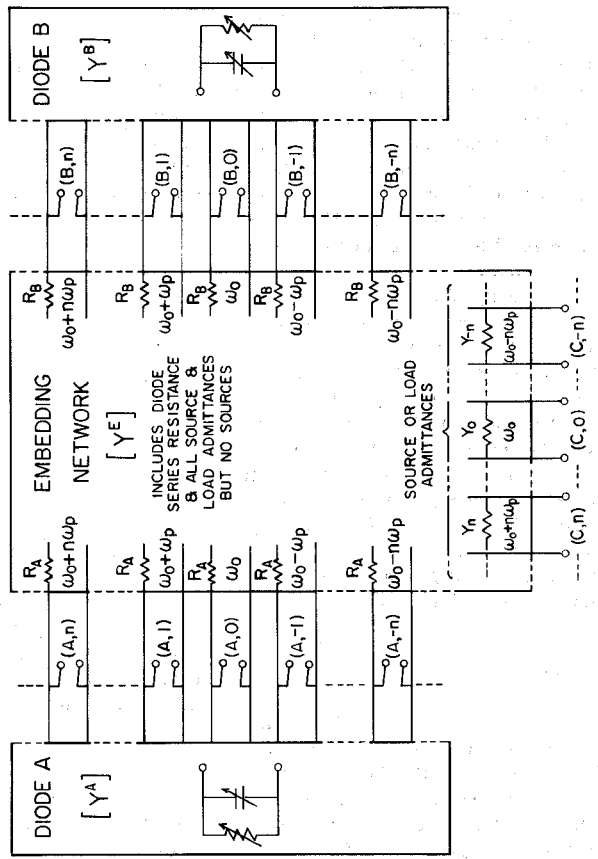


Fig. 2. Representation of the mixer as a multi-frequency multiport network. The embedding network contains the series resistance of the diodes and all source and load admittances Y_k connected externally to the diode mount. In normal mixer operation the ports shown in this diagram are all either open-circuited or connected to current sources at appropriate sideband frequencies. Port numbering (X, k) is such that $X = A, B$, or C if k is one of three faces of the embedding network, and k indicates sideband frequency $\omega_k = \omega_0 + k \omega_p$.